Integrating Glaucoma Endophenotypes Improves Polygenic Risk Prediction for Primary Open-Angle Glaucoma Across Ancestries

Xiaoyi Raymond Gao[1,2]

[1]Department of Ophthalmology and Visual Sciences, The Ohio State University, Columbus, OH 43210, USA

[2]Department of Biomedical Informatics, The Ohio State University, Columbus, OH 43210, USA

[*]Correspondence should be addressed to:
Xiaoyi Raymond Gao, PhD
Associate Professor
Department of Ophthalmology and Visual Sciences
Department of Biomedical Informatics
The Ohio State University
Columbus, OH 43212
USA
Phone: (614) 293-5287
Fax: (614) 293-5602
Email: raymond.gao@osumc.edu

Abstract

Primary open-angle glaucoma (POAG) is a leading cause of irreversible blindness, and early detection is crucial. Existing polygenic risk scores (PRSs) rely on single-trait models that lack the complementary genetic information captured by glaucoma endophenotypes. We developed a multi-trait polygenic probability risk score (PPRS) framework integrating trait-specific PRSs to improve prediction across ancestries. We evaluated the PPRS in the UK Biobank (n=324,713, European ancestry) and the Mexican American Glaucoma Genetic Study (MAGGS, n=4,549, Latino ancestry). Using SBayesRC with > 7 million variants and 96 functional annotations, we constructed PRSs for POAG, intraocular pressure (IOP), vertical cup-to-disc ratio (VCDR), and retinal nerve fiber layer thickness. Our PPRS combines these trait-specific PRSs via penalized logistic regression, preserving each trait's contribution. The PPRS achieved AUC values of 0.814 in Europeans and 0.802 in Latinos. Individuals in the highest PPRS decile had 74.4-fold (Europeans) and 49.3-fold (Latinos) higher odds of POAG than those in the lowest decile, with the top quintile capturing 65.7% and 62.2% of cases, respectively. Component trait contributions differed by ancestry: IOP PRS was strongest in Europeans (OR=1.63, $P = 5.37 \times 10^{-89}$), whereas VCDR PRS dominated in Latinos (OR=1.64, $P = 2.04 \times 10^{-11}$). Our multi-trait PPRS framework improves POAG prediction across ancestries and reveals that distinct endophenotypes drive genetic risk in different populations, supporting ancestry-informed risk stratification for targeted screening and earlier intervention. By decomposing polygenic risk into trait-specific components, this framework enables ancestry-informed glaucoma screening strategies that could facilitate earlier detection and personalized clinical management.

Keywords:

glaucoma, polygenic risk score, genetic prediction, diverse ancestry, risk stratification

Introduction

Glaucoma is the leading cause of irreversible blindness[1, 2], affecting about 80 million individuals worldwide[3, 4], with primary open-angle glaucoma (POAG) constituting approximately 90% of glaucoma cases in North America[4, 5]. Despite available treatments to slow disease progression, the irreversible nature of glaucoma-induced vision loss underscores the critical importance of early detection and intervention. While traditional risk assessment relies primarily on clinical measurements and family history, recent advances in genomics offer promising opportunities for enhanced risk stratification.

Polygenic risk scores (PRSs) have emerged as powerful tools for quantifying genetic predisposition to complex diseases[6-8]. However, their application to POAG has faced several key limitations. First, previous studies utilizing single-trait PRSs have achieved limited stratification ability, with only about 50% of cases being identified in the top PRS quintile in a recent report[9]. Second, existing approaches have limited capacity to capture the inherent complexity of POAG's pathophysiology, which involves multiple quantitative endophenotypes[1, 10], including intraocular pressure (IOP), vertical cup-to-disc ratio (VCDR), and retinal nerve fiber layer (RNFL) thickness. The multi-trait analysis of genome-wide association studies (MTAG) approach can increase power to detect associations by jointly analyzing genetically correlated traits; however, it assumes that all SNPs share the same variance-covariance matrix across traits, potentially leading to biased effect size estimates and an increased rate of false positives[11]. Third, most POAG PRS prediction studies have employed limited genomic coverage (< 1M markers) and have lacked integration of functional annotations. These limitations highlight the necessity for more sophisticated models that can capture the multifaceted genetic underpinnings of POAG.

Here, we present a multi-trait polygenic probability risk score (PPRS) approach that addresses these limitations through three key innovations: 1) integrating multiple disease-relevant quantitative traits into PRS modeling while preserving the individual contributions of each trait to enable interpretable, ancestry-

specific risk assessment; 2) incorporating extensive genomic coverage (> 7 million variants) and functional annotations; 3) validating across diverse ancestral populations. We hypothesized that this comprehensive approach would significantly improve POAG risk stratification across diverse populations compared to existing methods. To test this hypothesis, we evaluated our model in two independent cohorts: the UK Biobank (UKB) for European ancestry individuals and the Mexican American Glaucoma Genetic Study (MAGGS) for Latino participants.

Materials and Methods

Study Design and Populations

We conducted a two-stage study: first, deriving genome-wide association study (GWAS) summary statistics from previously published data and our own GWAS analyses (details provided below); second, constructing and evaluating PRSs in a subset of the UKB cohort (n = 324,713, POAG cases: 2,168) and the MAGGS cohort (n = 4,549, POAG cases: 275), both independent of the GWAS discovery samples. UKB was approved by the North West Multi-Center Research Ethics Committee[12, 13] and MAGGS was approved by the institutional review board at the University of Illinois at Chicago[14]. All participants provided written informed consent. The study adhered to the tenets of the Declaration of Helsinki. We obtained fully de-identified data to ensure participant confidentiality. We utilized the UKB and MAGGS datasets because both include genome-wide genotyping and detailed ophthalmic phenotypes suitable for glaucoma risk modeling. The UKB provided a large cohort enabling development and benchmarking of predictive models in participants of European ancestry, while MAGGS offered an independent Latino cohort for cross-ancestry evaluation.

UKB dataset

The UKB is an ongoing, large-scale prospective cohort study with over 500,000 adult participants aged 40 to 69 at enrollment (2006–2010), registered with the National Health Service in the United Kingdom[12, 13]. The study collected medical information and DNA samples, including ophthalmologic data for a subset

of approximately 118,000 participants. Our analysis focused on participants of European ancestry. Genotyping was performed using the UK BiLEVE Axiom Array or the UKB Axiom Array, with imputation based on reference panels from the 1000 Genomes Project (1KGP), UK10K, and the Haplotype Reference Consortium[15]. Variants with an imputation INFO score less than 0.3 and minor allele frequency less than 0.01 were excluded, resulting in approximately 10.3 million variants for downstream analysis. For individuals with IOP measurements, VCDR values, and RNFL data, we used previously published IOP GWAS results[16], VCDR summary statistics[17], and conducted a GWAS of RNFL to derive summary statistics. For those without ophthalmic exams (n = 324,713, unrelated, independent of the IOP, VCDR, and RNFL GWAS samples)[18], we utilized their data for PRS construction and association testing with POAG. Importantly, individuals contributing to the IOP, VCDR, and RNFL GWAS were distinct from those used as the target sample for PRS testing, ensuring no sample overlap. POAG (H40.1) cases were identified using the International Classification of Diseases Tenth Revision (ICD-10) codes. Controls were identified as those who did not have glaucoma.

MAGGS dataset

MAGGS samples were sourced from the Los Angeles Latino Eye Study (LALES)[19], a population-based epidemiologic study examining visual impairment and ocular diseases in 6,357 Latino individuals aged 40 or older in Los Angeles County, California. The presence of POAG was determined by agreement among three glaucoma specialists using clinical data, including the presence of open angles, characteristic visual field abnormalities, and optic disc damage in at least one eye. MAGGS and LALES genotyped 4,996 Latino individuals using either the Illumina OmniExpress BeadChip or the Illumina Hispanic/SOL BeadChip[14, 20]. Imputation was performed using 1KGP reference panel, excluding variants with a Mach[21] Rsq less than 0.3 and minor allele frequency less than 0.01, resulting in approximately 9.9 million imputed variants. Our analysis included 4,549 participants (4,108 unrelated and 441 related individuals) from this dataset.

GWAS summary statistics

We used previously published GWAS summary statistics for POAG, IOP, and vertical cup-to-disc ratio (VCDR), as well as our own GWAS results for RNFL. We primarily selected publicly available GWAS summary statistics with the largest available sample sizes at the time of analysis. When suitable public datasets were unavailable, we conducted in-house GWAS to generate summary statistics. This strategy ensured the use of the most comprehensive and up-to-date data for each phenotype. The details are as follows:

1) POAG: We used GWAS results from Gharahkhani et al. (2021), which performed a multi-ethnic meta-analysis using the International Glaucoma Genetics Consortium (IGGC) and UKB datasets, comprising 383,500 individuals of European, Asian, and African descent[22]. For building PRSs for UKB participants, we used results from IGGC only, excluding UKB individuals, resulting in a cross-ancestry meta-analysis with 192,702 individuals suitable for UKB PRS construction.

2) IOP: We used GWAS results from Gao *et al.* (2018), including 115,486 UKB participants of European ancestry[16].

3) VCDR: We used GWAS summary statistics from Han et al. (2021), involving 111,724 individuals of European and Asian descent from UKB, the Canadian Longitudinal Study on Aging (CLSA), and IGGC[17]. VCDR measurements were obtained from human graders and deep learning models applied to retinal fundus images.

4) RNFL: We conducted a GWAS with 52,902 European ancestry UKB participants using the REGENIE[23] software and RNFL thickness values derived from optical coherence tomography images[24]. We excluded outliers and low-quality images (image quality score less than 45). We averaged RNFL values between the left and right eyes and applied rank-based inverse normalization. We adjusted for age, sex, diabetes, spherical equivalent, and the first 10 principal components of genetic ancestry, as these factors are known to influence RNFL thickness or serve as potential confounders in genetic association studies. Supplementary Figure 1 presents a Manhattan plot of the genome-wide -log10(*P* values) for our RNFL GWAS analysis.

151 These summary statistics provided the foundation for constructing PRSs in our analysis, tailored to
152 different phenotypes relevant to POAG risk.
153
154 *PRS construction*
155 We employed three different approaches to construct PRSs:
156 First, we implemented a traditional clumping and thresholding (C+T) based PRS[25] using PLINK[26, 27]
157 to construct the POAG PRS, denoted as PRS-POAG-C+T. Independent single nucleotide polymorphisms
158 (SNPs) were identified using linkage disequilibrium (LD)-based clumping ($r^2 < 0.3$) and selected based
159 on a p-value threshold of $P < 5 \times 10^{-5}$.
160 Second, we constructed enhanced PRSs using the SBayesRC[28] method, which leverages functional
161 genomic annotations and extensive SNP coverage to improve polygenic risk prediction for complex traits
162 or diseases. By integrating 96 functional annotations, including regulatory elements, chromatin states, and
163 transcription factor binding sites, and analyzing over seven million SNPs, we sought to substantially im-
164 prove PRS accuracy. Using SBayesRC, we constructed PRSs for POAG (PRS-POAG), IOP (PRS-IOP),
165 VCDR (PRS-VCDR), and RNFL thickness (PRS-RNFL).
166 Third, we constructed a MTAG-derived PRS for POAG to enable direct comparison. We utilized
167 summary statistics for 2,763 uncorrelated SNPs (identified through LD clumping at $r^2 = 0.1$ and a signifi-
168 cance threshold of $P < 0.001$) from Craig *et al.*'s (2020) MTAG analysis[29]. The MTAG-derived PRS was
169 calculated using the formula: PRS-POAG-MTAG(i) = $\sum \beta_j G_{ij}$, where β_j represents the regression coeffi-
170 cient for SNP_j, and G_{ij} indicates the risk allele dosage for SNP_j in individual i. Since the MTAG summary
171 statistics were generated using UKB data, we avoided applying the MTAG-derived PRS to UKB partici-
172 pants to prevent data leakage. Consequently, this PRS was exclusively applied to MAGGS participants.
173
174 *Statistical analysis*
175 For testing the association between the PRSs and POAG, we carried out traditional logistic regression
176 analyses, adjusting for age and sex. All constructed PRSs were standardized to have a mean of zero and a

variance of one. To check potential multicollinearity among PRSs, we used two complementary approaches. First, we computed the variance inflation factor (VIF) for each predictor, noting that VIF values less than 5 typically indicate low correlation[30]. Second, we employed XGBoost[31], a tree-based method known to be less sensitive to collinearity, and examined feature importances via SHapley Additive exPlanations (SHAP) values[32], following our previous methodology[33].

For assessing the predictive ability of the PRSs for POAG, we used penalized (L2) logistic regression with stratified 10-fold cross-validation performed separately in the UKB and MAGGS datasets. We defined the polygenic probability risk score (PPRS) as the predicted probability output from an L2-penalized logistic regression model (scikit-learn LogisticRegression with penalty = "l2" [34]), which integrates four PRSs (PRS-POAG, PRS-IOP, PRS-VCDR, and PRS-RNFL) together with age and sex as covariates. The model takes these inputs and outputs a probability of glaucoma for each individual, which we term the PPRS. This formulation differentiates the PPRS from traditional single-trait PRSs and the MTAG-derived PRS. For MAGGS related samples, predictive models were developed using MAGGS unrelated samples and subsequently applied to the related individuals to derive predicted probabilities. We used the area under the receiver operating characteristic curve (AUC) to quantify the predictive ability of the PPRS on POAG. Pairwise comparisons of AUC between different models were performed using Delong's test[35]. For risk stratification, we divided the PPRS into deciles and compared the odds of POAG among study participants in higher PPRS deciles versus those in the lowest PPRS decile in both the UKB and MAGGS datasets. A statistical significance threshold of $P < 0.05$ was used for all analyses. All analyses were performed using R (v4.4; including the ggplot2 package for plotting), SAS 9.4 (SAS, Inc., Cary, NC, for non-penalized logistic regression), and Python (v3.12; scikit-learn for penalized logistic regression, XGBoost for gradient boosting models, and SHAP for model interpretability).

Results

Table 1 summarizes the characteristics of our study samples from UKB and MAGGS. The UKB cohort comprised 324,713 individuals with 2,168 glaucoma cases and 322,545 controls. The mean (standard deviation [SD]) age of glaucoma and non-glaucoma was 63.0 (5.7) and 57.1 (8.0) years, respectively. Females consisted of 48.4% of glaucoma cases and 54.3% of controls. The MAGGS dataset included 4,549 participants with 275 glaucoma cases and 4,274 controls. The mean (SD) age of glaucoma and non-glaucoma was 66.4 (11.1) and 56.1 (10.2), respectively. Females constituted 52.4% of glaucoma cases and 59.2% of controls.

Table 2 presents the single PRS association results (logistic regression analyses), adjusted for age and sex, among UKB and MAGGS participants. In the UKB cohort (Table 2a), the traditional clumping and thresholding (C+T) PRS for POAG (PRS-POAG-C+T) yielded an odds ratio (OR) of 1.71 (95% confidence interval [CI]: 1.64–1.79; $P = 8.71 \times 10^{-141}$). The SBayesRC-derived PRS for POAG (PRS-POAG, which integrates functional annotation information) showed a stronger association with an OR of 2.14 (95% CI: 2.05–2.24; $P = 8.54 \times 10^{-269}$). The SBayesRC-derived PRSs for IOP (PRS-IOP), VCDR (PRS-VCDR), and RNFL thickness (PRS-RNFL) also demonstrated significant associations with POAG. Similarly, in the MAGGS cohort (Table 2b), the PRS-POAG-MTAG had an OR of 1.44 (95% CI: 1.24–1.60; $P = 1.17 \times 10^{-7}$). PRS-VCDR showed the highest OR of 1.90 (95% CI: 1.66-2.17; $P = 1.39 \times 10^{-20}$). The PRS-POAG-C+T, PRS-IOP, PRS-POAG, and PRS-RNFL in MAGGS participants also exhibited significant associations with POAG.

Table 3 displays the results of the multiple PRS logistic regression analyses, assessing the combined association of PRSs with POAG and their relative importance in each cohort. In the UKB participants, PRS-POAG had an OR of 1.59 ($P = 1.23 \times 10^{-74}$), PRS-IOP showed the strongest association with an OR of 1.63 ($P = 5.37 \times 10^{-89}$), PRS-VCDR had an OR of 1.28 ($P = 1.99 \times 10^{-27}$), and PRS-RNFL exhibited an OR of 0.94 ($P = 0.002$), indicating a slight inverse association (larger PRS-RNFL indicated thicker

226 RNFL and hence is protective). The OR for a simultaneous one-SD-unit-increase in all four standardized
227 PRS variables was 3.11 (95% CI: 2.89-3.34). In the MAGGS cohort, PRS-POAG had an OR of 1.40 (P =
228 7.63×10^{-5}), PRS-IOP an OR of 1.15 (P = 0.07), PRS-VCDR showed the strongest association with an
229 OR of 1.64 ($P = 2.04 \times 10^{-11}$), and PRS-RNFL had an OR of 0.85 (P = 0.016), also suggesting an inverse
230 relationship. The OR for a simultaneous one-SD-unit-increase in all four standardized PRS variables was
231 2.25 (95% CI: 1.79-2.82). These results highlight ancestry-specific differences in genetic contributions to
232 POAG risk, with PRS-IOP contributing most significantly in the UKB dataset (European ancestry),
233 whereas PRS-VCDR had the strongest contribution in the MAGGS dataset (Latino ancestry). We further
234 evaluated potential collinearity among these PRSs using VIF (Supplementary Table 1) and XGBoost with
235 SHAP-based feature importance (Supplementary Figure 2). Both methods indicated no collinearity issues,
236 underscoring the robustness of our logistic regression analyses.
237
238 We then examined the discriminatory ability of the PRSs (PRS-POAG, PRS-IOP, PRS-VCDR, and
239 PRS-RNFL) for predicting POAG using penalized (L2) logistic regression with stratified 10-fold cross-
240 validation and calculated the area under the receiver operating characteristic curve (AUC). Figure 1 illus-
241 trates these results. In UKB participants (Figure 1A), the baseline model including only age and sex had
242 an AUC of 0.721 (95% CI: 0.711-0.730). Adding PRS-POAG-C+T increased the AUC to 0.761 (95% CI:
243 0.752-0.771), while incorporating the SBayesRC-derived PRS-POAG improved it to 0.790 (95% CI:
244 0.781-0.799), a 3% increase over the C+T approach ($P = 1.13 \times 10^{-29}$). Incorporating all four PRSs (PRS-
245 POAG, PRS-IOP, PRS-VCDR, and PRS-RNFL) with adjustment for age and sex resulted in an AUC of
246 0.814 (95% CI: 0.806–0.823), representing a 9.3% improvement over the baseline model ($P = 1.15 \times 10^{-}$
247 ^{112}) and a 2.1% improvement over the SBayesRC-derived PRS-POAG ($P = 6.25 \times 10^{-28}$). In MAGGS par-
248 ticipants (Figure 1B), the baseline AUC was 0.753 (95% CI: 0.724-0.782), which increased to 0.761 (95%
249 CI: 0.732-0.789) with PRS-POAG-MTAG, to 0.773 (95% CI: 0.744-0.802) with PRS-POAG-C+T, and to
250 0.782 (95% CI: 0.754-0.810) with PRS-POAG. The full model with all four PRSs (PRS-POAG, PRS-
251 IOP, PRS-VCDR, and PRS-RNFL) achieved an AUC of 0.802 (95% CI: 0.775–0.828), providing a 5%

252 enhancement over the baseline model ($P = 5.25 \times 10^{-6}$) and a 2% enhancement over the SBayesRC-de-
253 rived PRS-POAG ($P = 9.92 \times 10^{-4}$). These findings indicate that incorporating multiple glaucoma-related
254 PRSs significantly improves the prediction of POAG in both cohorts.
255
256 We further evaluated POAG risk stratification using polygenic probability risk score (PPRS), inte-
257 grating the effect of multiple PRSs of POAG, IOP, VCDR, and RNFL (with adjustment for age and sex),
258 from our penalized 10-fold cross-validation logistic regression models. Analysis of PPRS revealed strong
259 risk stratification capabilities (Figure 2). In the UKB cohort (Figure 2A), a clear trend emerged with in-
260 creasing ORs across higher PPRS deciles. Individuals in the highest decile had 74.35-fold increased odds
261 of POAG (95% CI: 43.87–126.02; $P = 1.28 \times 10^{-57}$) compared with those in the lowest decile, and 12.82-
262 fold increased odds (95% CI: 10.22–16.09; $P = 1.17 \times 10^{-107}$) compared with those in the 5th decile. Simi-
263 larly, in the MAGGS cohort (Figure 2B), participants in the highest decile demonstrated 49.34-fold in-
264 creased odds of POAG (95% CI: 15.54–156.62; $P = 3.69 \times 10^{-11}$) compared with the lowest decile and
265 9.61-fold increased odds (95% CI: 5.50–16.77; $P = 1.72 \times 10^{-15}$) compared with the 5th decile. Most
266 POAG cases (46.54% in UKB and 40.73% in MAGGS) fell within the highest decile category of PPRS
267 (Supplementary Table 2). Taken together, these findings underscore the strong relationship between
268 PPRS extreme deciles and POAG risk across UKB and MAGGS, highlighting the potential utility of the
269 PPRS for POAG risk stratification.
270
271 **Discussion**
272 Our study demonstrates that integrating multiple glaucoma-related traits with functional annotations sub-
273 stantially improves the polygenic prediction for POAG across diverse ancestries. Three key findings
274 emerge from our analysis: First, our multi-modal PPRS approach achieved higher predictive accuracy,
275 with AUC values of 0.814 (95% CI: 0.806–0.823) in Europeans and 0.802 (95% CI: 0.775–0.828) in Lati-
276 nos, compared to our POAG single-trait models. This improvement likely reflects the complex genetic
277 architecture of POAG, where multiple biological pathways contribute to disease development. Second,

278 we identified ancestry-specific differences in the relative contributions of component PRSs. In Europeans,
279 IOP showed the strongest association, whereas VCDR was most strongly associated in Latinos. This find-
280 ing underscores the importance of population-specific risk assessment and suggests distinct genetic mech-
281 anisms underlying POAG across ancestral groups. Third, the strong risk stratification achieved by our
282 PPRS, demonstrating over 74.4-fold and 49.3-fold risk differences between extreme deciles in Europeans
283 and Latinos, respectively, suggests significant clinical utility. Importantly, unlike approaches that collapse
284 multiple traits into a single combined score (e.g., via multi-trait analysis of GWAS), our framework pre-
285 serves trait-specific PRS contributions, enabling the identification of ancestry-specific differences in the
286 genetic architecture underlying POAG risk.
287
288 One of the most direct potential clinical applications of PRS is identifying high-risk individuals.
289 MacGregor et al. (2018), using an IOP PRS, reported an increased glaucoma risk (OR = 5.6, 95% CI:
290 4.1–7.6) comparing the top and bottom deciles[36]. Craig et al. (2020), employing an MTAG approach for
291 their POAG PRS, observed a higher OR of 14.9 (95% CI: 10.7–20.9) for comparing the top and bottom
292 deciles[29]. Gao et al. (2019) found an OR of 6.3 for their top IOP PRS quintile versus the bottom quintile
293 comparison, with approximately 40.6% of POAG cases found in the top quintile[18]. Similarly, de Vries et
294 al. (2025) identified about 50% of cases in their top glaucoma PRS quintile[9]. Our study substantially im-
295 proves upon these results, demonstrating ORs of 74.4 (95% CI: 43.9–126.0) in Europeans and 49.3 (95%
296 CI: 15.5–156.6) in Latinos when comparing extreme deciles of our PPRS. Additionally, we identified
297 65.7% and 62.2% of glaucoma cases within the top quintile of our PPRS scores for Europeans and Lati-
298 nos (Supplementary Table 2), respectively, representing a substantial improvement over previous studies.
299
300 While the improvement in AUC from the best single PRS (PRS-POAG, AUC = 0.790) to the full
301 PPRS model (AUC = 0.814) may appear modest in absolute terms (ΔAUC = 0.024), such increments are
302 consistent with prior reports in complex disease genetics and can nonetheless have important implications
303 in practice. In our study, the PPRS not only improved overall discrimination but also strengthened risk

separation at the extremes of the distribution, with substantially elevated odds of glaucoma observed in the top decile compared with the bottom decile. Most importantly, the full PPRS model identified 12.1% more cases in the top decile than the PRS-POAG model. These tail effects are clinically relevant for identifying individuals most likely to benefit from targeted surveillance or early intervention. We therefore view the statistically significant increment in AUC as both supportive of the additive value of integrating multiple glaucoma-related PRSs and a foundation for further improvement when combined with imaging, electronic health record, or other multimodal data in future predictive models.

The observation that PRS-IOP contributed most strongly to prediction in Europeans, whereas PRS-VCDR appeared more influential in Latinos, is intriguing but should be interpreted with caution. These differences may partly reflect disparities in sample size and statistical power across discovery GWAS. Cohort-specific factors such as recruitment differences, phenotype definitions, and environmental exposures may also have influenced the relative performance of the PRSs. Nevertheless, prior studies have shown that IOP PRS significantly improves discrimination for glaucoma in Europeans[18], and over 72% of known POAG risk loci are also associated with IOP in predominantly European datasets[22], underscoring the key role of IOP in POAG pathogenesis in this ancestry group. At the same time, epidemiological studies report variation in POAG presentation across populations[37]: in Latinos, the majority of cases occur with IOP < 21 mmHg, with elevated IOP (>21 mmHg) observed in only ~18% of cases. This pattern is consistent with stronger predictive value of VCDR-based genetic risk in the MAGGS cohort. The borderline non-significance of PRS-IOP in the MAGGS multiple regression model ($P = 0.07$) underscores the need for caution, as the limited sample size constrains power for precise estimates. Additional studies in larger and more diverse cohorts will be essential to further validate these ancestry-specific patterns.

Concurrent with our work, MacGregor *et al.*[38] developed a glaucoma PRS using SBayesRC and data from over 6 million individuals, including 23andMe participants, and demonstrated strong risk stratifica-

329 tion across five ancestry groups (European, African, East Asian, South Asian, and Admixed Ameri-
330 can/Hispanic) as well as clinical utility in predicting treatment escalation and surgical intervention. While
331 their approach achieves impressive performance through a substantially larger discovery sample and a
332 single combined MTAG-derived PRS, our multi-trait PPRS framework provides complementary and dis-
333 tinct insights. Specifically, by retaining separate trait-specific PRSs (for POAG, IOP, VCDR, and RNFL)
334 and combining them at the prediction model level, our approach reveals that the relative genetic contribu-
335 tions of these component traits differ across ancestries, with IOP contributing most strongly in Europeans
336 and VCDR in Latinos. This finding has implications for understanding the heterogeneous pathophysiol-
337 ogy of POAG across populations and for tailoring future risk assessment strategies. Moreover, the two
338 approaches are not mutually exclusive: incorporating our multi-trait integration framework with the larger
339 discovery datasets used by MacGregor *et al*. could further improve prediction accuracy and interpretabil-
340 ity in future work.
341
342 Our study has several strengths, notably the use of a comprehensive multi-trait PPRS approach that
343 integrates multiple glaucoma-related traits and leverages functional annotations to improve prediction ac-
344 curacy. By evaluating PRS performance in both European and Latino populations, we address the crucial
345 need for inclusive and representative genetic research, especially among traditionally understudied
346 groups[39]. However, our study also has limitations. Due to resource constraints, we included only Euro-
347 pean and Latino populations in this study. Expanding future research to additional ancestry populations
348 would enhance generalizability and ensure broader applicability of our findings. In addition, the smaller
349 sample size of the MAGGS Latino cohort limits the precision of effect estimates within this ancestry, un-
350 derscoring the need for replication in larger datasets. Furthermore, our PRS construction was limited to
351 common variants. Incorporating rare variants, similar to previous reports on rare variants associated with
352 IOP[40], warrants further investigation. Additionally, compared with recent large-scale efforts that leverage
353 discovery samples exceeding 6 million individuals, our GWAS discovery samples are substantially
354 smaller; however, the purpose of our study is to demonstrate the added value of a multi-trait integration

355 framework rather than to maximize single-trait PRS performance through sample size alone. Future stud-
356 ies combining our multi-trait approach with larger multi-ancestry discovery datasets may yield further im-
357 provements.
358
359 It is noteworthy that the MTAG-derived PRS did not outperform the single-trait GWAS PRS in our
360 analysis. Several factors likely contributed. First, we applied MTAG only to the MAGGS Latino samples,
361 where the smaller cohort size may limit stable estimation. Second, we constructed PRS using the state-of-
362 the-art SBayesRC framework, which leverages functional annotations to increase power. Finally, alt-
363 hough the recently published large-scale POAG MTAG GWAS[41] included >600,000 participants and
364 could potentially offer improved power, only p-values (and not SNP effect sizes) were released, preclud-
365 ing its direct use for PRS derivation in this study. Notably, our multi-trait PPRS approach circumvents the
366 limitations of MTAG by instead combining individual trait-specific PRSs at the prediction model level,
367 which avoids MTAG's assumption of a shared variance–covariance structure across all SNPs and enables
368 the assessment of differential trait contributions across ancestries.
369
370 In conclusion, our multi-trait PPRS approach, combining multiple glaucoma-related traits and incor-
371 porating functional annotations, represents a significant advancement in polygenic risk prediction for
372 POAG. By retaining trait-specific PRS contributions rather than collapsing them into a single score, our
373 framework uniquely reveals that the genetic determinants of POAG risk differ across ancestries, with
374 IOP-related genetic variation contributing most strongly in Europeans and VCDR-related variation in La-
375 tinos. The robust performance across different ancestral groups and substantial risk stratification capabili-
376 ties suggest considerable potential for enhancing early detection and preventative strategies. By facilitat-
377 ing the identification of individuals at high genetic risk, our approach has significant implications for
378 timely clinical intervention and could ultimately reduce the public health burden of POAG.
379
380

Acknowledgements

We would like to thank the study participants from the UK Biobank, the Los Angeles Latino Eye Study, the Mexican American Glaucoma Genetic Study, and the staff who aided in data collection and processing. This work was supported in part by National Institutes of Health (NIH; Bethesda, MD, USA) grants P30EY032857 and R01EY022651. The content is solely the responsibility of the authors and does not necessarily represent the official views of the NIH.

Author Contributions

X.R.G. conceived the present study, analyzed the data and wrote the manuscript.

Data availability statement

The SNP weight data used in this study are available at https://github.com/xraygao/PPRS.

Conflict of Interest Statement

None declared.

397 **References**

398 1. Fan BJ, Wiggs JL. Glaucoma: genes, phenotypes, and new directions for therapy. J Clin Invest
399 2010;120(9):3064-72.
400 2. Blindness GBD, Vision Impairment C, Vision Loss Expert Group of the Global Burden of
401 Disease S. Causes of blindness and vision impairment in 2020 and trends over 30 years, and prevalence of
402 avoidable blindness in relation to VISION 2020: the Right to Sight: an analysis for the Global Burden of
403 Disease Study. Lancet Glob Health 2021;9(2):e144-e60.
404 3. Weinreb RN, Leung CK, Crowston JG, et al. Primary open-angle glaucoma. Nat Rev Dis Primers
405 2016;2:16067.
406 4. Tham YC, Li X, Wong TY, et al. Global prevalence of glaucoma and projections of glaucoma
407 burden through 2040: a systematic review and meta-analysis. Ophthalmology 2014;121(11):2081-90.
408 5. Lang GK. Ophthalmology: A Pocket Textbook Atlas, 2nd ed. Stuttgart, New Yok: Thieme 2007.
409 6. Purcell SM, Wray NR, Stone JL, et al. Common polygenic variation contributes to risk of
410 schizophrenia and bipolar disorder. Nature 2009;460(7256):748-52.
411 7. Kachuri L, Chatterjee N, Hirbo J, et al. Principles and methods for transferring polygenic risk
412 scores across global populations. Nat Rev Genet 2024;25(1):8-25.
413 8. Torkamani A, Wineinger NE, Topol EJ. The personal and clinical utility of polygenic risk scores.
414 Nat Rev Genet 2018;19(9):581-90.
415 9. de Vries VA, Hanyuda A, Vergroesen JE, et al. The Clinical Usefulness of a Glaucoma Polygenic
416 Risk Score in 4 Population-Based European Ancestry Cohorts. Ophthalmology 2025;132(2):228-37.
417 10. Ramdas WD, Amin N, van Koolwijk LM, et al. Genetic architecture of open angle glaucoma and
418 related determinants. J Med Genet 2011;48(3):190-6.
419 11. Turley P, Walters RK, Maghzian O, et al. Multi-trait analysis of genome-wide association
420 summary statistics using MTAG. Nat Genet 2018;50(2):229-37.
421 12. Sudlow C, Gallacher J, Allen N, et al. UK biobank: an open access resource for identifying the
422 causes of a wide range of complex diseases of middle and old age. PLoS Med 2015;12(3):e1001779.
423 13. Allen NE, Sudlow C, Peakman T, et al. UK biobank data: come and get it. Sci Transl Med
424 2014;6(224):224ed4.
425 14. Nannini DR, Torres M, Chen YI, et al. A Genome-Wide Association Study of Vertical Cup-Disc
426 Ratio in a Latino Population. Invest Ophthalmol Vis Sci 2017;58(1):87-95.
427 15. Bycroft C, Freeman C, Petkova D, et al. The UK Biobank resource with deep phenotyping and
428 genomic data. Nature 2018;562(7726):203-9.
429 16. Gao XR, Huang H, Nannini DR, et al. Genome-wide association analyses identify new loci
430 influencing intraocular pressure. Hum Mol Genet 2018;27(12):2205-13.
431 17. Han X, Steven K, Qassim A, et al. Automated AI labeling of optic nerve head enables insights
432 into cross-ancestry glaucoma risk and genetic discovery in >280,000 images from UKB and CLSA. Am J
433 Hum Genet 2021.
434 18. Gao XR, Huang H, Kim H. Polygenic Risk Score Is Associated With Intraocular Pressure and
435 Improves Glaucoma Prediction in the UK Biobank Cohort. Transl Vis Sci Technol 2019;8(2):10.
436 19. Varma R, Paz SH, Azen SP, et al. The Los Angeles Latino Eye Study: design, methods, and
437 baseline data. Ophthalmology 2004;111(6):1121-31.
438 20. Nannini D, Torres M, Chen YD, et al. African Ancestry Is Associated with Higher Intraocular
439 Pressure in Latinos. Ophthalmology 2016;123(1):102-8.
440 21. Li Y, Abecasis GR. Mach 1.0: Rapid haplotype reconstruction and missing genotype inference.
441 Am J Hum Genet 2006;S79.
442 22. Gharahkhani P, Jorgenson E, Hysi P, et al. Genome-wide meta-analysis identifies 127 open-angle
443 glaucoma loci with consistent effect across ancestries. Nat Commun 2021;12(1):1258.
444 23. Mbatchou J, Barnard L, Backman J, et al. Computationally efficient whole-genome regression for
445 quantitative and binary traits. Nat Genet 2021;53(7):1097-103.

24. Ko F, Foster PJ, Strouthidis NG, et al. Associations with Retinal Pigment Epithelium Thickness Measures in a Large Cohort: Results from the UK Biobank. Ophthalmology 2017;124(1):105-17.
25. Prive F, Vilhjalmsson BJ, Aschard H, Blum MGB. Making the Most of Clumping and Thresholding for Polygenic Scores. Am J Hum Genet 2019;105(6):1213-21.
26. Purcell S, Neale B, Todd-Brown K, et al. PLINK: a tool set for whole-genome association and population-based linkage analyses. Am J Hum Genet 2007;81(3):559-75.
27. Chang CC, Chow CC, Tellier LC, et al. Second-generation PLINK: rising to the challenge of larger and richer datasets. Gigascience 2015;4:7.
28. Zheng Z, Liu S, Sidorenko J, et al. Leveraging functional genomic annotations and genome coverage to improve polygenic prediction of complex traits within and between ancestries. Nat Genet 2024;56(5):767-77.
29. Craig JE, Han X, Qassim A, et al. Multitrait analysis of glaucoma identifies new risk loci and enables polygenic prediction of disease susceptibility and progression. Nat Genet 2020;52(2):160-6.
30. James G, Witten D, Hastie T, Tibshirani R. An Introduction to Statistical Learning with Applications in R, 1st ed. New York, NY: Springer, 2009; 426 p.
31. Chen T, Guestrin C. XGBoost: A Scalable Tree Boosting System. Proceedings of the 22nd ACM SIGKDD International Conference on Knowledge Discovery and Data Mining. San Francisco, California, USA: Association for Computing Machinery, 2016.
32. Lundberg SM, Erion G, Chen H, et al. From local explanations to global understanding with explainable AI for trees. Nature Machine Intelligence 2020;2(1):56-67.
33. Gao XR, Chiariglione M, Qin K, et al. Explainable machine learning aggregates polygenic risk scores and electronic health records for Alzheimer's disease prediction. Scientific Reports 2023;13(1):450.
34. Pedregosa F, Varoquaux Gl, Gramfort A, et al. Scikit-learn: Machine Learning in Python. J Mach Learn Res 2011;12(null):2825–30 , numpages = 6.
35. DeLong ER, DeLong DM, Clarke-Pearson DL. Comparing the areas under two or more correlated receiver operating characteristic curves: a nonparametric approach. Biometrics 1988;44(3):837-45.
36. MacGregor S, Ong JS, An J, et al. Genome-wide association study of intraocular pressure uncovers new pathways to glaucoma. Nat Genet 2018;50(8):1067-71.
37. Varma R, Ying-Lai M, Francis BA, et al. Prevalence of open-angle glaucoma and ocular hypertension in Latinos: the Los Angeles Latino Eye Study. Ophthalmology 2004;111(8):1439-48.
38. MacGregor S, Ni G, Seviiri M, et al. Step change in glaucoma polygenic risk score performance enables clinical utility and disease prediction across all major ancestries. medRxiv 2026:2026.01.23.26344675.
39. Martschenko DO, Wand H, Young JL, Wojcik GL. Including multiracial individuals is crucial for race, ethnicity and ancestry frameworks in genetics and genomics. Nat Genet 2023;55(6):895-900.
40. Gao XR, Chiariglione M, Arch AJ. Whole-exome sequencing study identifies rare variants and genes associated with intraocular pressure and glaucoma. Nature Communications 2022;13(1):7376.
41. Han X, Gharahkhani P, Hamel AR, et al. Large-scale multitrait genome-wide association analyses identify hundreds of glaucoma risk loci. Nat Genet 2023;55(7):1116-25.

488 **Figure legends**

489 **Figure 1. Receiver Operating Characteristic Curves Predicting POAG Using Polygenic Risk Scores**

490 Receiver operating characteristic curves illustrating the predictive performance of polygenic risk scores
491 (PRSs) for primary open-angle glaucoma (POAG) in (A) the UK Biobank cohort and (B) the Mexican
492 American Glaucoma Genetic Study (MAGGS) cohort. In both cohorts, models incorporating age, sex,
493 and multi-trait PRSs significantly improved the area under the curve (AUC) compared to the baseline
494 models (age and sex only) and single-PRS models. Analysis was performed using penalized (L2) logistic
495 regression with stratified 10-fold cross-validation.

496 Abbreviations: IOP, intraocular pressure; RNFL, retinal nerve fiber layer; VCDR, vertical cup-to-disc ra-
497 tio.

498

499 **Figure 2. Association Between Polygenic Probability Risk Score Deciles and POAG Risk**

500 Odds ratios (ORs) for primary open-angle glaucoma (POAG) across deciles of the polygenic probability
501 risk score (PPRS) in (A) the UK Biobank cohort and (B) the Mexican American Glaucoma Genetic Study
502 (MAGGS) cohort. The fifth decile (Decile 5) serves as the reference group. Error bars represent 95% con-
503 fidence intervals (CIs). A clear trend of increasing POAG risk with higher PPRS deciles demonstrates
504 strong risk stratification capabilities of PPRS in both ancestral cohorts.

505
506

507 **Table 1. Sample Characteristics**
508

	UK Biobank (n = 324,713)		**MAGGS** (n = 4,549)	
	Controls (322,545)	Cases (2,168)	Controls (4,274)	Cases (275)
Age (yrs, SD)	57.1 (8.0)	63.0 (5.7)	56.1 (10.2)	66.4 (11.1)
Female (%)	54.3	48.4	59.2	52.4

509 Abbreviation: MAGGS, Mexican American Glaucoma Genetic Study; SD: standard deviation.
510
511

512 **Table 2. Single-PRS Logistic Regression Results**
513
514 (a) UK Biobank participants

	OR (95% CI)	*P* value
PRS-POAG-C+T	1.71 (1.64, 1.79)	8.71×10^{-141}
PRS-POAG	2.14 (2.05, 2.24)	8.54×10^{-269}
PRS-IOP	2.08 (2.00, 2.17)	1.04×10^{-248}
PRS-VCDR	1.61 (1.54, 1.68)	9.50×10^{-107}
PRS-RNFL	0.92 (0.89, 0.96)	2.52×10^{-4}

515 (b) MAGGS[†] participants

	OR (95% CI)	*P* value
PRS-POAG-C+T	1.64 (1.44, 1.88)	1.68×10^{-13}
PRS-POAG-MTAG	1.44 (1.24, 1.60)	1.17×10^{-7}
PRS-POAG	1.82 (1.59, 2.08)	2.79×10^{-18}
PRS-IOP	1.45 (1.27, 1.65)	1.66×10^{-8}
PRS-VCDR	1.90 (1.66, 2.17)	1.39×10^{-20}
PRS-RNFL	0.85 (0.74, 0.96)	0.011

516 Results of single-PRS logistic regression analyses, adjusted for age and sex. [†]Unrelated MAGGS partici-
517 pants (n = 4,108) were used. PRS-POAG, PRS-IOP, PRS-VCDR, and PRS-RNFL were SBayesRC-de-
518 rived. To prevent potential data leakage, MTAG-derived PRS (based on Craig et al.'s summary statistics,
519 which used UK Biobank data) was not applied to UK Biobank participants. PRS-POAG-MTAG was ex-
520 clusively applied to MAGGS study participants.

521 Abbreviations: C+T, clumping and thresholding; IOP, intraocular pressure; MAGGS, Mexican American
522 Glaucoma Genetic Study; OR, odds ratio; PRS, polygenic risk score; POAG, primary open-angle glau-
523 coma; RNFL, retinal nerve fiber layer thickness; VCDR, vertical cup-to-disc ratio.
524
525

526 **Table 3. Multiple Logistic Regression Results**
527

	UK Biobank		MAGGS†	
	OR (95% CI)	*P* value	OR (95% CI)	*P* value
PRS-POAG	1.59 (1.51, 1.67)	1.23×10^{-74}	1.40 (1.18, 1.65)	7.63×10^{-5}
PRS-IOP	1.63 (1.55, 1.71)	5.37×10^{-89}	1.15 (0.99, 1.35)	0.07
PRS-VCDR	1.28 (1.23, 1.34)	1.99×10^{-27}	1.64 (1.42, 1.90)	2.04×10^{-11}
PRS-RNFL	0.94 (0.90, 0.98)	0.002	0.85 (0.74, 0.97)	0.016

528 Results of multiple logistic regression analyses, adjusted for age and sex, assessing the combined associa-
529 tion of polygenic risk scores (PRSs) with primary open-angle glaucoma. †Unrelated MAGGS participants
530 (n = 4,108) were used. PRS-POAG, PRS-IOP, PRS-VCDR, and PRS-RNFL were SBayesRC-derived.

531 Abbreviations: IOP, intraocular pressure; MAGGS, Mexican American Glaucoma Genetic Study; OR,
532 odds ratio; PRS, polygenic risk score; POAG, primary open-angle glaucoma; RNFL, retinal nerve fiber
533 layer thickness; VCDR, vertical cup-to-disc ratio.
534
535

536 **Figure 1. Receiver Operating Characteristic Curves Predicting POAG Using Polygenic Risk Scores**

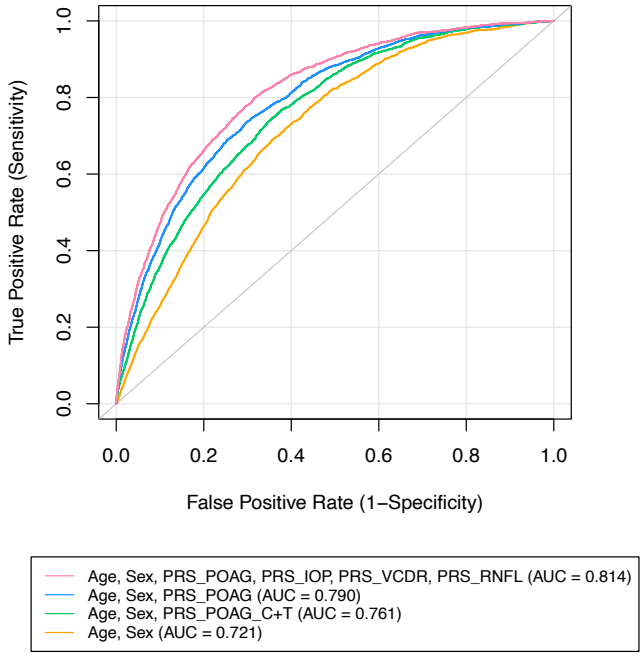

537
538 (a) UK Biobank participants

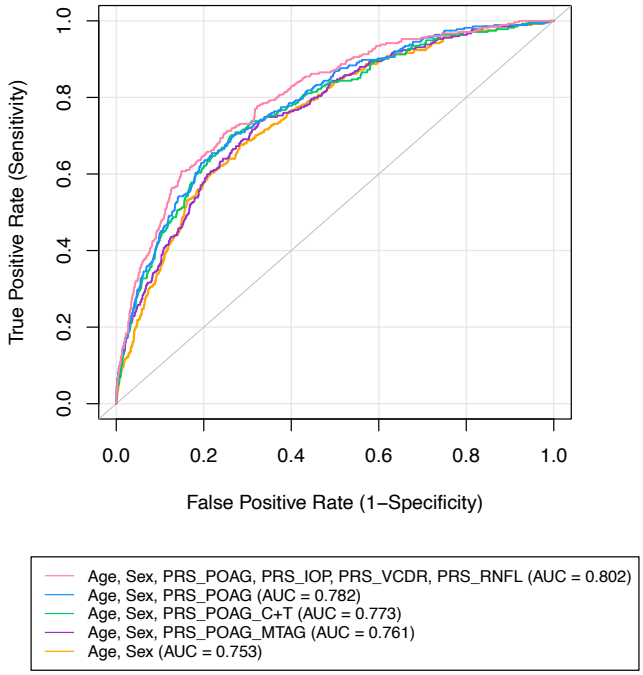

539
540 (b) MAGGS participants

541
542 **Figure 2. Association Between Polygenic Probability Risk Score Deciles and POAG Risk**

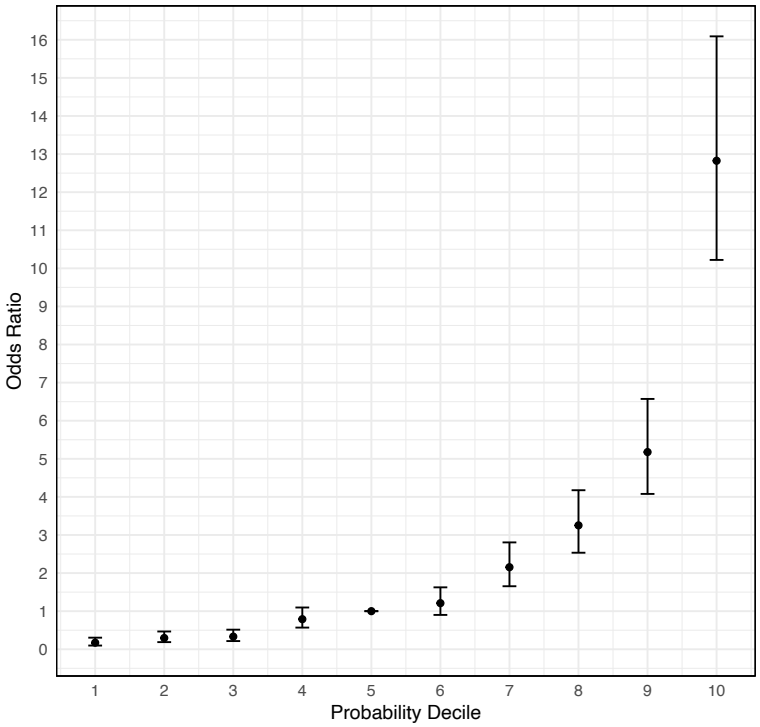

543
544 (a) UK Biobank participants

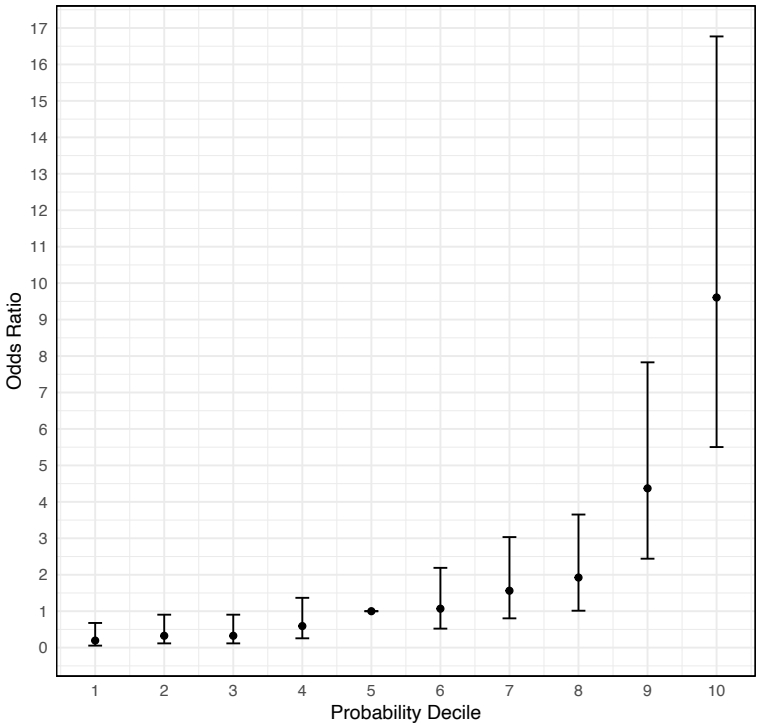

545
546 (b) MAGGS participants

Supplementary Table 1. Variance Inflation factors for polygenic risk scores in our logistic regression models

(a) UK Biobank

Age	Sex	PRS-POAG	PRS-IOP	PRS-VCDR	PRS-RNFL
1.002	1.002	1.347	1.240	1.112	1.003

(b) MAGGS[†]

Age	Sex	PRS-POAG	PRS-IOP	PRS-VCDR	PRS-RNFL
1.024	1.006	1.555	1.371	1.166	1.004

Displayed are the variance inflation factors for the polygenic risk scores (PRSs) used in our logistic regression analyses of a) UK Biobank; b) MAGGS. [†]Unrelated MAGGS participants were used. PRS-POAG, PRS-IOP, PRS-VCDR, and PRS-RNFL were SBayesRC-derived. These variant inflation factor values are only slightly above 1 and all remain well below the typical cutoff of 5, indicating no collinearity issues.

Abbreviations: IOP, intraocular pressure; MAGGS, Mexican American Glaucoma Genetic Study; PRS, polygenic risk score; POAG, primary open-angle glaucoma; RNFL, retinal nerve fiber layer thickness; VCDR, vertical cup-to-disc ratio.

Supplementary Table 2. Number of POAG Cases in Each Decile Category

(a) UK Biobank

	Predicted Probability Risk Score Decile									
	1	2	3	4	5	6	7	8	9	10
POAG, n (%)	14 (0.65)	24 (1.11)	27 (1.25)	64 (2.95)	81 (3.74)	98 (4.52)	174 (8.03)	262 (12.08)	415 (19.14)	1009 (46.54)

(b) MAGGS

	Predicted Probability Risk Score Decile									
	1	2	3	4	5	6	7	8	9	10
POAG, n (%)	3 (1.09)	5 (1.82)	5 (1.82)	9 (3.27)	15 (5.45)	16 (5.82)	23 (8.36)	28 (10.18)	59 (21.45)	112 (40.73)

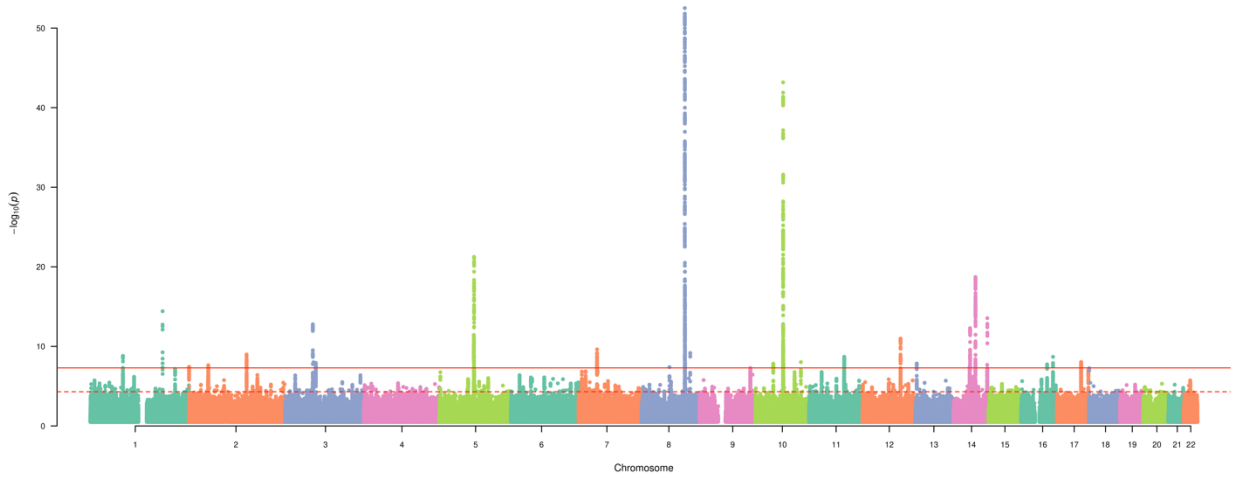

Supplementary Figure 1. Manhattan Plot Displaying the –log10(*P* values) for the Association Between RNFL Thickness and Genome-wide Genetic Variants

Solid and dotted horizontal lines represent genome-wide significant associations ($P < 5 \times 10^{-8}$) and suggestive associations ($P < 5 \times 10^{-5}$), respectively. Genetic variants are plotted by chromosomal position.

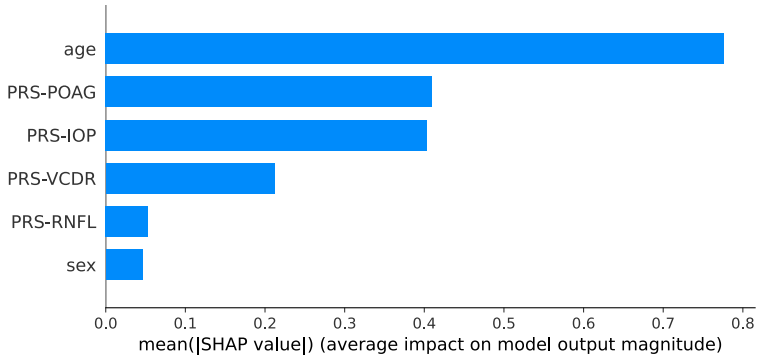

(a) UK Biobank participants

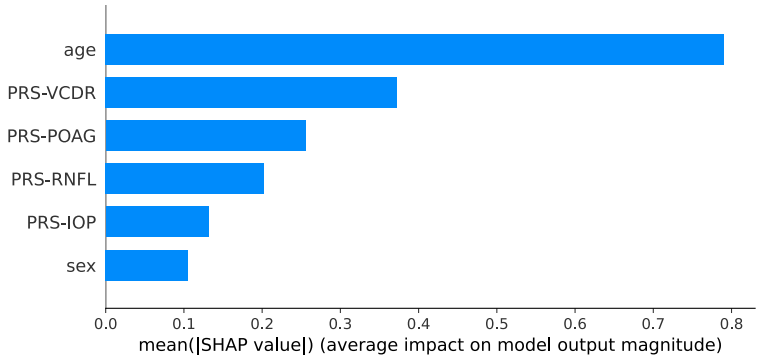

(b) MAGGS participants

Supplementary Figure 2. SHAP Feature Importance for XGBoost Models

Bar charts illustrating feature importance, as evaluated via SHapley Additive exPlanations (SHAP) values, for the (A) UK Biobank and (B) Mexican American Glaucoma Genetic Study (MAGGS) cohorts. The y-axis displays the ranked features, and the x-axis shows the average impact on the model's output. All PRSs (PRS-POAG, PRS-IOP, PRS-VCDR, and PRS-RNFL) were SBayesRC-derived. In UKB participants (European ancestry), PRS-IOP and PRS-POAG both rank highly among the PRSs, whereas in MAGGS participants (Latino ancestry), PRS-VCDR shows the highest importance among the PRSs. These results align with the logistic regression findings, confirming ancestry-specific differences in genetic contributions to POAG risk.

Abbreviations: IOP, intraocular pressure; RNFL, retinal nerve fiber layer; VCDR, vertical cup-to-disc ratio.